IOP Publishing Physica Scripta
Phys. Scr. **T140** (2010) 014018 (4pp) doi:10.1088/0031-8949/2010/T140/014018

Characterization of bipartite Gaussian states from OPO

V D'Auria[1], S Fornaro[2], A Porzio[2], S Solimeno[2,3], S Olivares[4,5] and M G A Paris[4,5]

[1] Laboratoire Kastler Brossel, Ecole Normale Supérieure, Université Pierre et Marie Curie, CNRS, 4 place Jussieu, 75252 Paris, France
[2] Dipartimento di Scienze Fisiche Università 'Federico II', Napoli, Italy
[3] CNISM UdR Napoli Università, Napoli, Italy
[4] CNISM UdR Milano Università, I-20133 Milano, Italy
[5] Dipartimento di Fisica dell'Università degli Studi di Milano, I-20133 Milano, Italy

E-mail: stefano.olivares@mi.infn.it

Received 29 March 2010
Accepted for publication 17 June 2010
Published 30 September 2010
Online at stacks.iop.org/PhysScr/T140/014018

Abstract
In a recent paper by D'Auria *et al* (2009 *Phys. Rev. Lett.* **102** 020502) we reported the full experimental reconstruction of Gaussian entangled states generated by a type-II optical parametric oscillator (OPO) below threshold using a single homodyne detector. Here we investigate more deeply the Gaussian character of the OPO output addressing the homodyne traces. More precisely, we apply a suitable normality test to check the actual Gaussian distribution of the homodyne data and then we perform the full reconstruction of the signal.

PACS numbers: 03.67.Mn, 03.65.Wj, 03.67.Bg, 42.65.Yj

(Some figures in this article are in colour only in the electronic version.)

1. Introduction

Light beams endowed with non-classical correlations [1, 2] are key ingredients for quantum technology and find applications in quantum communication [3], imaging [4] and precision measurement [5, 6]. Among others, entangled states produced by optical parametric oscillators (OPOs) are Gaussian states [7, 8] and thus may be fully characterized by the first two statistical moments of the field modes. In turn, the covariance matrix (CM) contains complete information about entanglement [9, 10], i.e. about their performances as a resource for quantum technology. Their full characterization is of fundamental interest on its own and represents a tool for the design of quantum information processing protocols in realistic conditions.

Recently, we presented the full experimental reconstruction of Gaussian entangled states generated by a type-II OPO below threshold [11]. The reconstruction setup was based on a single homodyne detector and we demonstrated the convenience and robustness of this method for the full characterization of OPO signals. Nevertheless, under particular conditions, OPO outputs may present non-Gaussian behaviours [12, 13]: in these scenarios a preliminary check on the Gaussian character of the signal under investigation is extremely important.

In this paper, the full reconstruction of the CM associated with OPO states is preceded with the analysis of its Gaussian character by applying a suitable normality test to the homodyne data.

2. Reconstruction method: the theory

This section briefly reviews the reconstruction method [14]. The CM $\boldsymbol{\sigma}$ of a bipartite state ϱ can be written as the block matrix:

$$\boldsymbol{\sigma} = \left(\begin{array}{c|c} A & C \\ \hline C^T & B \end{array} \right), \tag{1}$$

A, B and C being 2×2 real matrices. The entries of $\boldsymbol{\sigma}$ are given by $\sigma_{hk} = \frac{1}{2}\langle\{R_k, R_h\}\rangle - \langle R_k\rangle\langle R_h\rangle$, where $\langle O\rangle = \mathrm{Tr}[\varrho\, O]$ and $\{f, g\} = fg + gf$ is the anti-commutator; we also introduced the vector $\boldsymbol{R} = (x_1, y_1, x_2, y_2)$ of canonical operators in terms of the field mode operators a_k, $x_k = (a_k^\dagger + a_k)/\sqrt{2}$, $y_k = \mathrm{i}(a_k^\dagger - a_k)/\sqrt{2}$, $k = 1, 2$. From the CM of Gaussian states follow all their properties, such as positivity of the density matrix, state purity and separability [2].

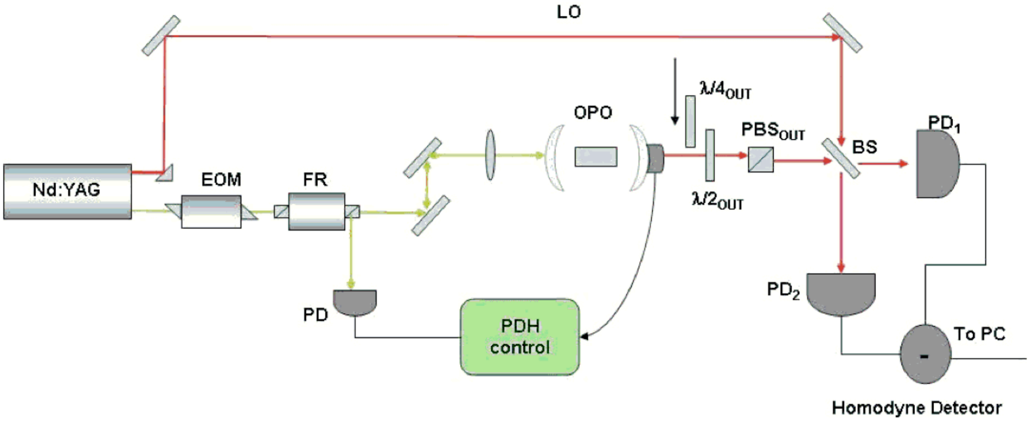

Figure 1. Experimental setup: a type-II OPO containing a periodically poled crystal (PPKTP) is pumped by the second harmonic of a Nd:YAG laser. At the OPO output, a half-wave plate ($\lambda/2_{\rm out}$), a quarter-wave plate ($\lambda/4_{\rm out}$) and a $PBS_{\rm out}$ select the mode for homodyning. The resulting electronic signal is acquired via a PC module.

Our reconstruction method considers the four additional auxiliary modes $c = (a+b)/\sqrt{2}$, $d = (a-b)/\sqrt{2}$, $e = (\mathrm{i}a+b)/\sqrt{2}$ and $f = (\mathrm{i}a-b)/\sqrt{2}$ obtained by the action of polarizing beam splitters (PBSs) and phase shifters on modes $a \equiv a_1$ and $b \equiv a_2$. In our experiment, block A of the CM is retrieved by measuring the single-mode quadratures of mode a: the variances of x_a and y_a give the diagonal elements, while the off-diagonal ones are obtained from the additional quadratures $z_a \equiv (x_a + y_a)/\sqrt{2}$ and $t_a \equiv (x_a - y_a)/\sqrt{2}$ as $\sigma_{12} = \sigma_{21} = \frac{1}{2}(\langle z_a^2\rangle - \langle t_a^2\rangle) - \langle x_a\rangle\langle y_a\rangle$ [14]. Block B is reconstructed in the same way from the quadratures of b, whereas the elements of block C are obtained from the quadratures of the auxiliary modes c, d, e and f as follows:

$$\sigma_{13} = \frac{1}{2}(\langle x_c^2\rangle - \langle x_d^2\rangle) - \langle x_a\rangle\langle x_b\rangle, \quad (2)$$

$$\sigma_{14} = \frac{1}{2}(\langle y_e^2\rangle - \langle y_f^2\rangle) - \langle x_a\rangle\langle y_b\rangle, \quad (3)$$

$$\sigma_{23} = \frac{1}{2}(\langle x_f^2\rangle - \langle x_e^2\rangle) - \langle y_a\rangle\langle x_b\rangle, \quad (4)$$

$$\sigma_{24} = \frac{1}{2}(\langle y_c^2\rangle - \langle y_d^2\rangle) - \langle y_a\rangle\langle y_b\rangle. \quad (5)$$

Notice that the measurement of the f-quadratures is not mandatory, since $\langle x_f^2\rangle = \langle x_b^2\rangle + \langle y_a\rangle^2 - \langle x_e^2\rangle$ and $\langle y_f^2\rangle = \langle x_a^2\rangle + \langle y_b^2\rangle - \langle y_e^2\rangle$. Analogous expressions hold for $\langle x_e^2\rangle$ and $\langle y_e^2\rangle$.

3. Reconstruction method: the experiment

3.1. Experimental setup

The experimental setup, shown in figure 1, is thoroughly described in [11]. In order to select modes a and b, coming from the OPO crystal, or their combinations c and d, the OPO beams are sent to a half-wave plate and a PBS. Modes e and f are obtained by inserting an additional quarter-wave plate [14]. The PBS output goes to a homodyne detector, described in detail in [6, 12], exploiting the laser output at 1064 nm as the local oscillator (LO). The overall homodyne detection efficiency is $\eta = 0.88 \pm 0.02$. The LO reflects on a piezo-mounted mirror (PZT), which allows variation of its phase θ. In order to avoid the laser low-frequency noise, data sampling is moved away from the optical carrier frequency by mixing the homodyne current with a sinusoidal signal of frequency $\Omega = 3$ MHz [12]. The resulting current is low-pass filtered ($B = 300$ kHz) and sampled by a PCI acquisition board (Gage 14100, 1M points per run, 14-bit resolution). The total electronic noise power was measured to be 16 dB below the shot-noise level, corresponding to a signal-to-noise ratio of about 40.

Acquisition is triggered by a linear ramp applied to the PZT and adjusted to obtain a 2π variation in 200 ms. Upon spanning the LO phase θ, the quadratures $x(\theta) = x\cos\theta + y\sin\theta$ are measured. Calibration with respect to the noise of the vacuum state is obtained by acquiring a set of data with the output from the OPO obscured. All the expectation values needed to reconstruct $\boldsymbol{\sigma}$ are obtained by quantum tomography [15], which allows one to compensate non-unit quantum efficiency and to reconstruct any expectation value, including those of specific quadratures and their variances, by averaging special pattern functions over the whole data set. As a preliminary check of the procedure, we verified that the CM of the vacuum state is consistent with $\boldsymbol{\sigma}_0 = \frac{1}{2}\mathbb{I}$ within experimental error.

3.2. Check on the OPO output Gaussian character

We start our analysis by checking the Gaussian character of the OPO signals, i.e. testing the Gaussianity of the homodyne distribution at fixed phase of the LO [12]. To this aim, we divided the homodyne traces into bins of ≈ 5000 data and applied the Shapiro–Wilk normality test [16] to each bin: if the p-value associated with the test exceeds the threshold value 0.05, then the null hypothesis (namely, the data are normally distributed) is true. In figure 2, we show the experimental homodyne traces for modes a, b, c and d (plots on the left) as well as the corresponding p-value of the Shapiro–Wilk test (plots on the right). As is apparent from the plots, both modes c and d are squeezed with quadrature noise reduction, corrected for non-unit efficiency, of about 2.5 dB for mode c and 2.8 dB for mode d. Analogous behaviour was observed for modes e and f.

In addition, we checked that the mean values of all the involved quadratures are negligible, in agreement with the

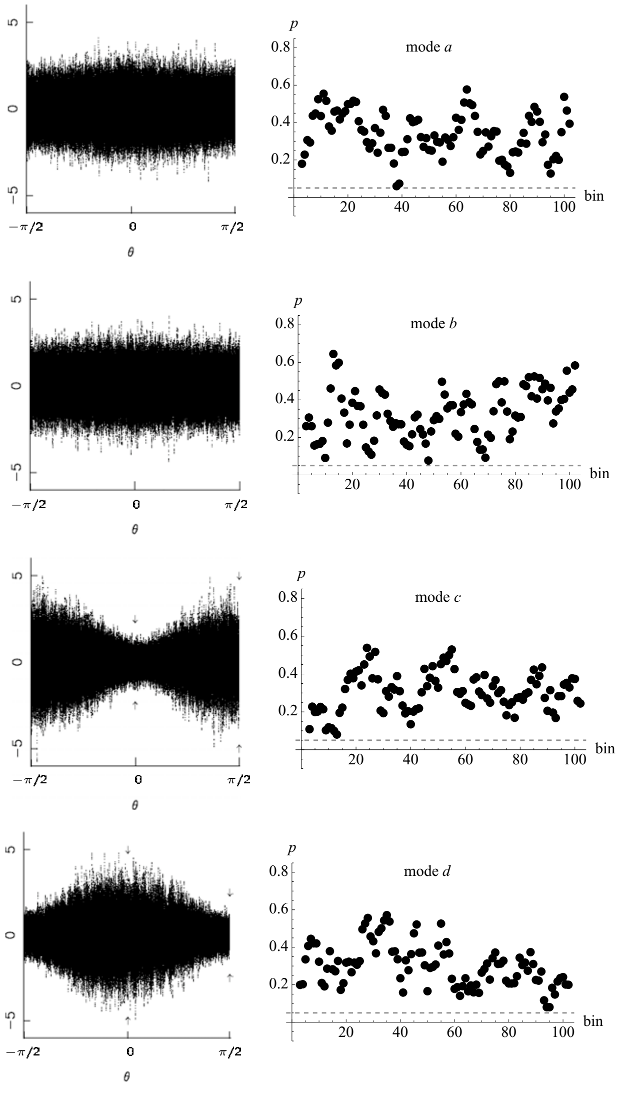

Figure 2. Left: from top to bottom, experimental homodyne traces of modes a, b, c and d. Right: p-value of the Shapiro–Wilk normality test as a function of bin number (see the text for details). Since we have p-values $\geqslant 0.05$ (the dashed line in the plots), we can conclude that our data are normally distributed. θ is the relative phase between the signal and the LO.

description of OPO output as a zero-amplitude state. Then, we measured the needed quadratures of the six modes a–f. We found modes a and b excited in a thermal state, thus confirming the absence of relevant local squeezing. Their combinations c, d, e and f are squeezed thermal states with squeezing appearing on y_c, x_d, t_e and z_f, respectively.

3.3. Experimental results and OPO state characterization

The reconstructed CM reads

$$\boldsymbol{\sigma} = \begin{pmatrix} 1.406 & 0.000 & 1.200 & 0.076 \\ 0.000 & 1.406 & 0.021 & -1.219 \\ 1.200 & 0.021 & 1.380 & 0.000 \\ 0.076 & -1.219 & 0.000 & 1.380 \end{pmatrix}. \quad (6)$$

It is worth noting that, in the ideal case, the OPO output is in a twin-beam state $\mathbf{S}(\zeta)|0\rangle$, $\mathbf{S}(\zeta) = \exp\{\zeta a^\dagger b^\dagger - \zeta^* ab\}$ being the entangling two-mode squeezing operator: the corresponding CM has diagonal blocks A, B, C with the two diagonal elements of each block equal in absolute value. In realistic OPOs, the state at the output is expected to be a zero-amplitude Gaussian entangled state, whose general form may be written as [11, 17]

$$\varrho_g = \mathbf{S}(\zeta)\,\mathbf{U}(\beta)\,\mathbf{LS}(\xi_1,\xi_2)\,\mathbf{T}\,\mathbf{LS}^\dagger(\xi_1,\xi_2)\,\mathbf{U}^\dagger(\beta)\,\mathbf{S}^\dagger(\zeta), \quad (7)$$

where $\mathbf{T} = \tau_1 \otimes \tau_2$, with $\tau_k = (1+\bar{n}_k)^{-1}[\bar{n}_k/(1+\bar{n}_k)]^{a^\dagger a}$, denotes a two-mode thermal state with $\bar{n}_k$ average photons per mode, $\mathbf{LS}(\xi_1,\xi_2) = S(\xi_1)\otimes S(\xi_2)$, $S(\xi_k) = \exp\{\frac{1}{2}(\xi_k a^{\dagger 2} - \xi_k^* a^2)\}$, denotes local squeezing and $\mathbf{U}(\beta) = \exp\{\beta a^\dagger b - \beta^* a b^\dagger\}$ is a mixing operator, ζ, ξ_k and β being complex numbers. For our configuration, besides a thermal contribution due to internal and coupling losses, we expect a relevant entangling contribution with a small residual local squeezing and, as mentioned above, a possible mixing among the modes. In the present case, the relevant parameters to characterize the density matrix ϱ_g corresponding to CM (2) are the mean number of thermal photons $\bar{n}_1 \simeq 0.25$, $\bar{n}_2 \simeq 0.13$ and entangling photons $\bar{n}_s = 2\sinh^2|\zeta| \simeq 1.02$ (the other parameters are given by $\zeta \simeq 0.66\,\mathrm{e}^{-\mathrm{i}\,0.04}$, $\xi_1 \simeq 0.03\,\mathrm{e}^{-\mathrm{i}\,0.41\pi}$, $\xi_2 \simeq 0.04\,\mathrm{e}^{\mathrm{i}\,0.38\pi}$, $\beta \simeq 0.68\,\mathrm{e}^{\mathrm{i}\,0.39\pi}$). A few considerations should be made about uncertainties on the CM elements. With respect to blocks A, B, and σ_{13} and σ_{24} of block C, uncertainties are of the order $\delta\sigma_{jk} \simeq 0.003$ and were obtained by propagating tomographic errors [11]. In all the previous cases the phase fluctuations are irrelevant, since the two modes a and b are both excited in a thermal state and the elements σ_{13} and σ_{24} are retrieved as combinations of squeezed/anti-squeezed variances, which are quite insensitive to fluctuations of θ. On the other hand, the elements σ_{14} and σ_{23} of block C depend on the determination of $x_{e,f}^2$ and $y_{e,f}^2$, which are sensible to phase fluctuations. Now, the resulting uncertainties are about $\delta\sigma_{14} = \delta\sigma_{23} \simeq 0.02$ for both CM elements, and are induced by a $\delta\theta \simeq 20$ mrad variation in the LO phase, corresponding to the experimental phase stability of the homodyne detection.

Starting from CM $\boldsymbol{\sigma}$, we can fully characterize our state. Since the minimum symplectic eigenvalue of $\boldsymbol{\sigma}$ is $\nu_- = 0.66 \pm 0.02 \geqslant 0.5$, the CM corresponds to a physical state with purity $\mu(\boldsymbol{\sigma}) = (4\sqrt{\mathrm{Det}[\boldsymbol{\sigma}]})^{-1} = 0.53 \pm 0.01$. The minimum symplectic eigenvalue for the partial transpose is $\tilde{\nu}_- = 0.18 \pm 0.02$, which corresponds to a logarithmic negativity $E_{\mathcal{N}}(\boldsymbol{\sigma}) = 1.01 \pm 0.02$, i.e. the state is entangled [18], with entanglement of formation $E_{\mathcal{F}}(\boldsymbol{\sigma}) = 1.28 \pm 0.02$ [19]. In turn, it satisfies the Duan inequality [10] with the results $0.37 \pm 0.01 < 2.00$ and the EPR criterion [20] with $0.12 \pm 0.01 < 1/4$.

In figure 3, we also report the single-mode photon distributions (either from data or from the single-mode CM) for modes a, b, c and d: distributions of a and b are thermal, whereas the statistics of modes c and d correctly reproduce the even–odd oscillations expected for squeezed thermal states.

4. Concluding remarks

We presented the full reconstruction of the CM of a bipartite state generated by an OPO below threshold following the method proposed in [14] and demonstrated in [11]. In particular, we faced the relevant problem of the actual Gaussian character of the state under investigation, which

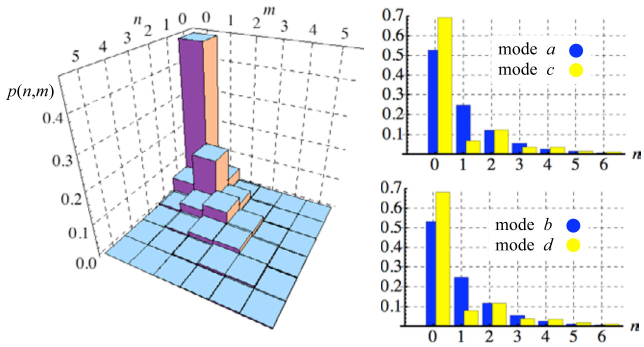

Figure 3. Left: joint photon number distribution $p(n, m)$ for the entangled state of modes a and b at the output of the OPO. Right: single-mode photon distributions $p(n)$ for modes a and c (top right) and b and d (bottom right). The single-mode distributions of modes a and b are thermal and correspond to the marginals of $p(n, m)$. The distributions of modes c and d are those of squeezed thermal states.

is assumed as a requirement by the reconstruction method. To this aim, we applied the Shapiro–Wilk normality test to the homodyne traces. We have shown that the state outgoing the OPO is a Gaussian state, and we have reconstructed its CM and obtained its main properties, such as purity and separability/entanglement.

Acknowledgments

Discussions with J Řehàček, Z Hradil and A Messina are acknowledged. This work was partially supported by the CNR–CNISM convention.

References

[1] Eisert J *et al* 2003 *Int. J. Quantum Inf.* **1** 479
Adesso G *et al* 2007 *J. Phys. A: Math. Theor.* **40** 7821
Braunstein S L *et al* 2005 *Rev. Mod. Phys.* **77** 513
[2] Ferraro A, Olivares S and Paris M G A 2005 *Gaussian States in Quantum Information* (Napoli: Bibliopolis) arXiv:0503237 [quant-ph]
[3] van Loock P 2002 *Fort. Phys.* **50** 1177
[4] Lugiato L A *et al* 2002 *J. Opt.* B **4** S176
[5] D'Ariano G M *et al* 2001 *Phys. Rev. Lett.* **87** 270404
[6] D'Auria V *et al* 2006 *J. Phys.* B **39** 1187
[7] Simon R *et al* 1987 *Phys. Rev.* A **36** 3868
Simon R *et al* 1994 *Phys. Rev.* A **49** 1567
[8] Marian P *et al* 1993 *Phys. Rev.* A **47** 4474
Marian P *et al* 1993 *Phys. Rev.* A **47** 4487
Marian P *et al* 2003 *Phys. Rev.* A **68** 062309
[9] Simon R 2000 *Phys. Rev. Lett.* **84** 2726
[10] Duan L-M *et al* 2000 *Phys. Rev. Lett.* **84** 2722
[11] D'Auria V *et al* 2009 *Phys. Rev. Lett.* **102** 020502
[12] D'Auria V *et al* 2005 *Opt. Express* **13** 948
[13] Řehàček J *et al* 2009 *Phys. Rev.* A **79** 032111
[14] D'Auria V *et al* 2005 *J. Opt. B: Quantum Semiclass. Opt.* **7** 750
Porzio A *et al* 2007 *Int. J. Quantum Inf.* **5** 63
[15] D'Ariano G M *et al* 2003 *Adv. Imaging Electron Phys.* **128** 205
[16] Shapiro S S and Wilk M B 1965 *Biometrika* **52** 591
Royston P 1995 *Appl. Stat.* **44** 547
[17] D'Auria V *et al* 2008 *Appl. Phys.* B **91** 309
[18] Vidal G *et al* 2002 *Phys. Rev.* A **65** 032314
[19] Marian P and Marian T A 2008 *Phys. Rev. Lett.* **101** 220403
[20] Treps N *et al* 2005 *Laser Phys.* **15** 187–94